Elastic $\alpha+^{20}$Ne scattering in the $\alpha+^{16}$O model of ^{20}Ne

Yong-Xu Yang,[1,*] Hai-Lan Tan,[1] and Qing-Run Li[2]
[1]*Department of Physics, Guangxi Normal University, Guilin 541004, China*
[2]*Institute of High Energy Physics, Chinese Academy of Sciences, Beijing 100039, China*
(Received 9 April 2010; published 19 August 2010)

A folding potential for the elastic $\alpha+^{20}$Ne scattering is constructed based on the $\alpha+^{16}$O structure model of the ^{20}Ne nucleus. The elastic scattering angular distributions of the $\alpha+^{20}$Ne system at incident energies $E_\alpha = 31.1$, 54.1, and 104.0 MeV have been calculated by using the folding potential. The experimental angular distributions and the anomalous large angle scattering (ALAS) features can be satisfactorily described. The anomaly of the $\alpha+^{20}$Ne system is clearly reconfirmed in the present folding model analysis and should be further systematically investigated.

DOI: 10.1103/PhysRevC.82.024607 PACS number(s): 25.70.Bc, 24.10.Ht, 21.60.Gx, 25.55.Ci

I. INTRODUCTION

The elastic α-nucleus scattering was extensively studied in the past. The α scattering on some light and medium-heavy nuclei exhibit strong enhancement of cross section at backward angles [i.e., the so-called anomalous large angle scattering (ALAS)]. This phenomenon brought considerable interest and was explained by various approaches (e.g., modified Woods-Saxon potential, L-dependent potential, folding potential, α exchange, Regge poles, and so on [1–12]).

For the elastic $\alpha+^{20}$Ne scattering, there have been the measured differential cross sections over complete angular range: in the lower incident energy region, the angular distributions at $E_\alpha = 16.8$ MeV [3], 18.0 MeV [4], 20.2–23.0 MeV [5], and 25.8–31.1 MeV [6]; in higher incident energy region, the very detailed measured angular distribution at $E_\alpha =$ 54.1 MeV [7]. All these experimental angular distributions exhibit remarkable ALAS features. In Ref. [6], the elastic $\alpha+^{20}$Ne scattering at incident energies of 25.8, 27.0, and 31.1 MeV have been analyzed in terms of a single Regge pole [by adding a Regge pole S_l(Reg) to the optical model S matrix S_l(diff), the two complex parameters were obtained from best fits to the data], and good fits to the experimental data were obtained. In Ref. [7], Abele *et al.* have calculated the $\alpha+^{20}$Ne elastic angular distribution at incident energy 54.1 MeV by using the DDM3Y folding potential, but obtained a very poor description to the experimental data. Michel and Reidemeister [8] have systematically analyzed the 54.1-MeV angular distribution using both parity-independent and parity-dependent potentials. It is shown that the parity-independent potentials were unable to obtain a satisfactory phasing with the data on the whole angular range, whereas the data can be quantitatively described by the introduction of a very small parity splitting in the real part of the interaction.

Because ALAS is especially pronounced for α scattering on $A = 4N$, α-particle nuclei, it implies that α cluster might play a role. From the point of view of the nuclear cluster structure, the ^{20}Ne nucleus is constructed with two clusters of α and ^{16}O. In the present work, basing on this viewpoint, we will construct a folding potential for the analysis of elastic $\alpha+^{20}$Ne scattering and do an examination for this nuclear structure model.

In the second section we present a brief outline of the formulas of the $\alpha+^{16}$O model of the ^{20}Ne nucleus, the $\alpha+^{16}$O relative motion wave function, and the folding model potential for the description of elastic $\alpha+^{20}$Ne scattering. The comparisons of calculations with the experimental data and discussions for the elastic $\alpha+^{20}$Ne scattering, by using the folding model potential, are given in the last section.

II. BRIEF PRESENTATION OF THE $\alpha+^{16}$O MODEL OF THE ^{20}Ne NUCLEUS AND THE FOLDING MODEL POTENTIAL FOR THE $\alpha+^{20}$Ne SCATTERING

From the point of view of the $\alpha+^{16}$O cluster structure of the ^{20}Ne nucleus, the real part of the optical potential for the $\alpha+^{20}$Ne scattering can be represented by the folding potential:

$$V(\mathbf{R}) = \int \left[V_{\alpha\alpha}\left(\mathbf{R} - \frac{4}{5}\mathbf{r}\right) + V_{\alpha^{16}\mathrm{O}}\left(\mathbf{R} + \frac{1}{5}\mathbf{r}\right)\right] |\chi_0(\mathbf{r})|^2 d\mathbf{r}, \tag{1}$$

where $\chi_0(\mathbf{r})$ is the wave function for the relative motion of the α and ^{16}O clusters in the ground state of the ^{20}Ne nucleus, and $\mathbf{r}$ is the relative coordinate between the centers of mass of α and ^{16}O.

For the α-α interaction $V_{\alpha\alpha}$, we use the potential given by Buck *et al.* [13], that is,

$$V_{\alpha\alpha}(r) = -122.6225 \exp(-0.22r^2)\ \mathrm{MeV}. \tag{2}$$

This potential can accurately reproduce the measured α-α scattering phase shifts for center-of-mass energies up to 20 MeV and approximately reproduce the experimental data for energies up to 40 MeV.

For the α-^{16}O interaction $V_{\alpha^{16}\mathrm{O}}$, we have constructed an α-folding model potential for the $\alpha+^{16}$O scattering [14]. This potential has an analytical and simple form, and can satisfactorily describe the experimental angular distributions of the elastic $\alpha+^{16}$O scattering at incident energies between

*yyxu@mailbox.gxnu.edu.cn

25 and 54 MeV. Thus this α-^{16}O potential can be well used to perform the α+^{20}Ne folding potential of expression (1).

The α+^{16}O relative motion wave function $\chi_0(\mathbf{r})$ in Eq. (1) can be obtained from the α+^{16}O model of the ^{20}Ne nucleus. In our recent article [15], we have proposed an α+^{16}O model of the ^{20}Ne nucleus. This model can very well reproduce the experimental charge form factor of ^{20}Ne and the elastic proton-^{20}Ne scattering differential cross sections. Based on this model, the relative motion wave function for the ground state of the ^{20}Ne nucleus can be written as

$$\chi_0(\mathbf{r}) = R_0(r)Y_{00}(\theta,\phi), \tag{3}$$

where $R_0(r)$ is the radial wave function and normalized as $\int R_0^2(r)r^2dr = 1$, and $Y_{lm}(\theta,\phi)$ is the spherical harmonic function. $R_0(r)$ can be expanded by means of a set of complete and orthogonal functions as

$$R_0(r) = \sum_{n=1}^{\infty} C_n \mathrm{O}_{n0}(r). \tag{4}$$

Here C_n is the expansion coefficient, and $\mathrm{O}_{nl}(r)$ is the harmonic oscillator radial function with principal quantum number n and angular momentum l.

By fitting the experimental charge form factor of ^{20}Ne, we obtained

$$R_0(r) = \mathrm{Sin}\frac{\theta}{2}\mathrm{O}_{10}(r) + \mathrm{Cos}\frac{\theta}{2}\mathrm{O}_{20}(r), (0 \leqslant \theta \leqslant 2\pi), \tag{5}$$

where $\mathrm{O}_{10}(r)$ and $\mathrm{O}_{20}(r)$ are the harmonic oscillator radial functions with the quantum numbers $1s$ and $2s$, respectively, that is,

$$\mathrm{O}_{10}(r) = 2(a^6\pi)^{-\frac{1}{4}} e^{-\frac{r^2}{2a^2}}, \tag{6}$$

and

$$\mathrm{O}_{20}(r) = \sqrt{\frac{8}{3}}(a^6\pi)^{-\frac{1}{4}}\left[\frac{3}{2} - \left(\frac{r}{a}\right)^2\right] e^{-\frac{r^2}{2a^2}}. \tag{7}$$

The obtained parameters are $a = 1.96$ fm and $\theta = 282.4^\circ$.

The wave function of expression (4) has the analytical and simple form. This is a significant advantage that makes it feasible and convenient to perform calculation of the α+^{20}Ne folding model potential of Eq. (1). Now from the analytical and simple forms of the $V_{\alpha\alpha}$, $V_{\alpha^{16}\mathrm{O}}$, and χ_0, the folding model potential (1) can be easily obtained and expressed as an analytical function.

As usual folding model calculations, the total optical potential used to describe the elastic α+^{20}Ne scattering is the form as

$$U(R) = NV(R) + W(R) + V_C(R), \tag{8}$$

where N is the renormalization factor, $W(R)$ is the imaginary part of the interaction, and $V_C(R)$ is the Coulomb interaction. The Coulomb potential $V_C(R)$ used in our calculations is usually taken to correspond to the uniformly charged sphere of radius $R_C = 1.3A^{1/3}$.

For the imaginary part of the interaction between the incident α particle and the target nucleus, we take the standard Woods-Saxon form,

$$W(R) = \frac{-iW_0}{1 + \exp(\frac{R-R_W}{a_W})}, \tag{9}$$

with $R_W = r_W A^{1/3}$.

III. RESULTS AND DISCUSSION

Among the available experimental angular distributions of the elastic α+^{20}Ne scattering, the data at 54.1 MeV is the most interested and attended one. The authors of Ref. [7] have measured the differential cross sections over complete angular range for 54.1 MeV α elastic scattering on 10 nuclei from ^{11}B to ^{24}Mg. Scanning these measured angular distributions, one can notice that the angular distribution for ^{20}Ne has a quite different behavior from those for the nearby targets ^{18}O, ^{17}O, ^{16}O, and the lighter targets ^{15}N, ^{14}N, ^{13}C. For the targets ^{18}O, ^{17}O, ^{16}O, ^{15}N, ^{14}N, and ^{13}C, the angular distributions display analogical patterns and are "normal": displaying a midangle broad plateau followed by a rainbowlike exponential falloff at larger angles. In contrast, the angular distribution for ^{20}Ne shows remarkable ALAS [7]. And more unexpected, the analyses for these measured angular distributions by Abele *et al*. [7] show that the DDM3Y folding potential which works well for the region of medium-heavy nuclei, can successfully describe the data for targets ^{18}O, ^{17}O, ^{16}O, ^{15}N, ^{14}N, and ^{13}C, but is completely failed to describe the data of ^{20}Ne. Their calculated result for ^{20}Ne is shown as the dashed line in Fig. 1 here, convenient for review.

As the main work of this article, we firstly investigate the 54.1-MeV α elastic scattering on ^{20}Ne using the folding potential constructed in Sec. II. The calculated angular distribution is shown in Fig. 1. The corresponding values of the parameters by fitting the data are $N = 1.14$, $W_0 = 22.5$ MeV, $r_W = 1.65$ fm, and $a_W = 0.60$ fm. From Fig. 1, one can see that successful description for this data is obtained by the

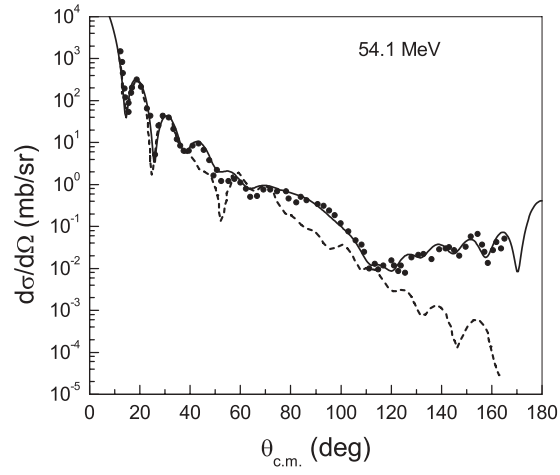

FIG. 1. The angular distribution of elastic α+^{20}Ne scattering at incident energy $E_\alpha = 54.1$ MeV. The solid curve is the result from our folding model potential with a standard Woods-Saxon imaginary part. The dashed curve displays the result from the DDM3Y folding potential in Ref. [7].

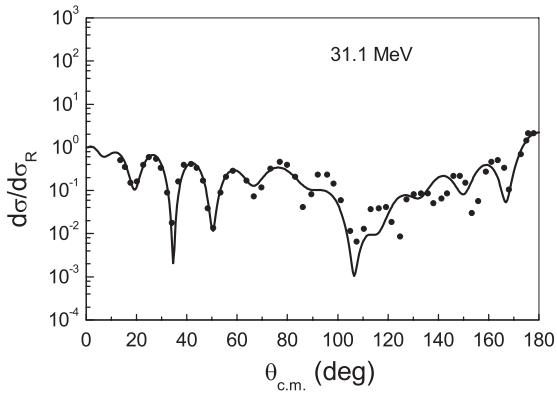

FIG. 2. The same as Fig. 1 but the differential cross section as a ratio to Rutherford at the incident energy $E_\alpha = 31.1$ MeV. The data are from Ref. [6].

present α-folding potential. The intention of the present work is to examine the $\alpha+^{16}$O model of the ^{20}Ne nucleus by means of the elastic $\alpha+^{20}$Ne scattering. For further examination, we extend this α-folding potential to the lower incident energy region, where the ALAS feature was observed, and the higher incident energy region. Here, we choose the data of $E_\alpha = 31.1$ and 104.0 MeV for further analysis. To see the dominant effect of the model, we simplify the imaginary potential by reducing the free parameters. In the following calculations we take the parameters r_W and a_W as fixed values of 1.65 and 0.60 fm obtained previously, with only N and W_0 as the varying parameters to obtain the fit to the experimental data. The calculated angular distributions for incident energies $E_\alpha = 31.1$ and 104.0 MeV are, respectively, shown in Figs. 2 and 3. The corresponding values of the parameters are listed in Table I. One can see that for higher incident energy $E_\alpha = 104.0$ MeV, the quality of the fit is very good. In the case of the lower incident energy $E_\alpha = 31.1$ MeV, the magnitude and trend of the variation of the cross section with the scattering angle, especially the behavior of the remarkable backward rising, have been well reproduced, but detailed fits to the experimental data at the back angle region are discrepant. These inaccurate fits result from the use of the oversimplified imaginary potential with only one parameter

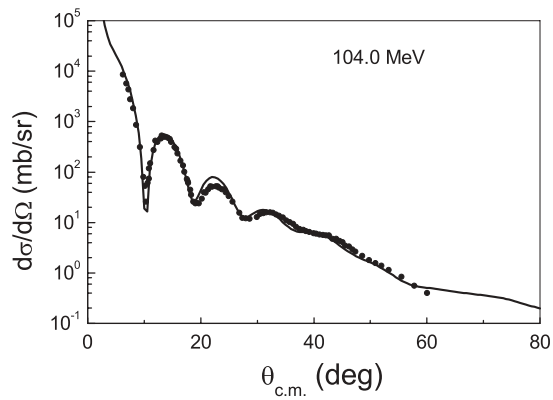

FIG. 3. The same as Fig. 1 but at the incident energy $E_\alpha = 104.0$ MeV. The data are from Ref. [16].

TABLE I. Values of the renormalization factor, the central depth of the imaginary potential, and the volume integrals of the real and the imaginary potential.

E_α (MeV)	N	W_0 (MeV)	$J_R/4A$ (MeV·fm^3)	$J_I/4A$ (MeV·fm^3)
31.1	1.08	17.0	446.8	94.1
54.1	1.14	22.5	471.6	124.6
104.0	1.18	29.0	488.2	160.6

W_0 adjustable. As is well known, the quality of the fit can be significantly improved by increasing the flexibility of the imaginary potential. For instance, we can choose an imaginary potential as a sum of Fourier-Bessel functions with six adjustable parameters as used in Ref. [7], or a generally used form of a volume absorption term plus a surface absorption term with six parameters. As an example, Fig. 4 shows the result for $E_\alpha = 31.1$ MeV by using the imaginary potential of a Woods-Saxon (WS) volume term plus a surface term of a Woods-Saxon derivative (WSD) shape. The parameters of N, W_0, r_W, a_W, W_D, r_D, and a_D were adjusted to optimize the fit to the experimental data. One can see from Fig. 4 that, with an imaginary potential of a Woods-Saxon volume term plus a surface term, our folding potential can get a very satisfactory fit to the experimental data. As mentioned above, it is not the intention of the present article to find the optimum fit to the experimental data for each individual incident energy, but to get an examination for the $\alpha+^{16}$O model of the ^{20}Ne nucleus. For this aim, the quality of the fits shown in Figs. 1–3, calculated by our folding model potential with an imaginary potential of a standard Woods-Saxon type, should be considered as good as the $\alpha+^{16}$O model of the ^{20}Ne nucleus that has been examined well.

In our calculations, the required renormalization factors are $N \approx 1.14 \pm 0.06$. The obtained volume integrals for the real potential $J_R/4A$ are about from 450 to 490 MeV·fm^3 and for the imaginary potential $J_I/4A$ are from 90 to 160 MeV·fm^3 (see Table I). The volume integrals of the real potential show very weakly dependent on energy in this incident energy

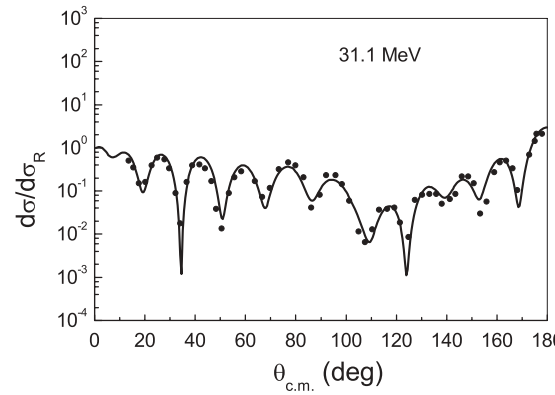

FIG. 4. The same as Fig. 2 but for an imaginary potential of the sum of a Woods-Saxon volume term and a surface term of a Woods-Saxon derivative shape.

range, whereas the imaginary part is found to be increased with increasing energy. It should be pointed out that, with the required renormalization factor $N \approx 1.14$ which is about 14% discrepant to unity and is acceptable, the obtained volume integral $J_R/4A \approx 472$ MeV·fm^3 is "anomalous," stronger compared to those of "normal" potentials for lower mass targets. Analyses [7,8,17,18] have shown that, for α scattering on some lower mass targets, a real potential with volume integral $J_R/4A$ around 350 MeV·fm^3 can well reproduce the experimental cross sections. For the case of the 54.1-MeV elastic $\alpha+^{16}$O scattering, in our previous calculation by using the α-folding model [14], the required renormalization factor is $N = 0.82$ which gives a "normal" value of the volume integral of the real potential $J_R/4A = 340$ MeV·fm^3. Here, we see the anomaly of the $\alpha+^{20}$Ne scattering, which was revealed in the analyses in Refs. [7,8].

From the analyses by Abele *et al.* in Ref. [7], a question was revealed: why the "normal" folding model works well for a series of light nuclei but completely fails for the ^{20}Ne nucleus? This problem was systematically investigated by Michel and Reidemeister [8]. At first, using phenomenological potentials, they found that the real potentials with volume integral $J_R/4A$ in excess of about 500 MeV·fm^3, which is much stronger than those of "normal" potentials for lower mass targets, can produce the backward angle enhancement for the 54.1-MeV elastic $\alpha+^{20}$Ne scattering, but is unable to obtain a complete fit to the data for whole angular range. Our present calculated result is accordant with this conclusion. The present folding potential with $J_R/4A = 472$ MeV·fm^3 can get a good fit to the 54.1-MeV data shown in Fig. 1, but one can see the phasing difference of the calculations from the experimental data at the backward angle. Further investigations by Michel and Reidemeister [8] have shown that, using a real potential with $J_R/4A$ about 350 MeV·fm^3 similar to those for neighboring mass targets, plus a small parity-dependent real part, a precise agreement with the experimental angular distribution was obtained. These analyses provide a possible answer to the "anomaly" of elastic $\alpha+^{20}$Ne scattering. However, as is pointed out in Ref. [8], the origin of the parity dependence is not clear at this stage. And as far as we know there is no evidence for the requirement to introduce the parity dependence to the interaction for neighboring light targets. The "anomaly" of ^{20}Ne target is still an inexplicit problem for us and further systematic investigation should be done to make it clear.

In summary, based on the $\alpha+^{16}$O model of the ^{20}Ne nucleus, we have constructed a folding model potential to describe the elastic $\alpha+^{20}$Ne scattering. This folding potential, with a simple Woods-Saxon type imaginary part, can satisfactorily describe the experimental angular distributions of the elastic $\alpha+^{20}$Ne scattering for a wide incident energy region, and especially can well reproduce the ALAS features. The anomaly of the $\alpha+^{20}$Ne scattering is clearly reconfirmed in the present analysis and should be further studied.

ACKNOWLEDGMENTS

The research is supported by National Natural Science Foundation of China under Grant No. 10865002.

[1] K. W. McVoy, Phys. Rev. C **3**, 1104 (1971).
[2] D. Agassi and N. S. Wall, Phys. Rev. C **7**, 1368 (1973).
[3] J. W. Frickey, K. A. Eberhard, and R. H. Davis, Phys. Rev. C **4**, 434 (1971).
[4] L. Seidlitz, E. Bleuler, and D. J. Tendam, Phys. Rev. **110**, 682 (1958).
[5] J. B. A. England, E. Casal, A. Garcia, T. Picazo, J. Aguilar, and H. M. Sen Gupta, Nucl. Phys. A **284**, 29 (1977).
[6] A. A. Cowley, J. C. Van Staden, S. J. Mills, P. M. Cronje, G. Heymann, and G. F. Burdzik, Nucl. Phys. A **301**, 429 (1978).
[7] H. Abele *et al.*, Z. Phys. A **326**, 373 (1987).
[8] F. Michel and G. Reidemeister, Z. Phys. A **333**, 331 (1989).
[9] A. S. B. Tariq, A. F. M. M. Rahman, S. K. Das, A. S. Mondal, M. A. Uddin, A. K. Basak, H. M. Sen Gupta, and F. B. Malik, Phys. Rev. C **59**, 2558 (1999).
[10] F. Michel, S. Ohkubo, and G. Reidemeister, Prog. Theor. Phys. Suppl. **132**, 7 (1998).
[11] K. E. Rehm *et al.*, Phys. Rev. Lett. **89**, 132501 (2002).
[12] M. N. A. Abdullah *et al.*, Nucl. Phys. A **760**, 40 (2005).
[13] B. Buck, H. Friedrich, and C. Wheathly, Nucl. Phys. A **275**, 246 (1977).
[14] Q. R. Li and Y. X. Yang, Nucl. Phys. A **561**, 181 (1993).
[15] P. T. Ong, Y. X. Yang, and Q. R. Li, Eur. Phys. J. A **41**, 229 (2009).
[16] H. Rebel, G. W. Schweimer, J. Specht, G. Schatz, R. Löhken, D. Habs, G. Hauser, and H. Klewe-Nebenius, Phys. Rev. Lett. **26**, 1190 (1971).
[17] F. Michel, J. Albinski, P. Belery, Th. Delbar, Gh. Gregoire, B. Tasiaux, and G. Reidemeister, Phys. Rev. C **28**, 1904 (1983).
[18] T. Furumoto and Y. Sakuragi, Phys. Rev. C **74**, 034606 (2006).